KeAi
CHINESE ROOTS
GLOBAL IMPACT

Available online at www.sciencedirect.com

ScienceDirect

Advances in Climate Change Research 12 (2021) 18–28

www.keaipublishing.com/en/journals/accr/

Permafrost change in Northeast China in the 1950s–2010s

ZHANG Zhong-Qiong[a,*], WU Qing-Bai[a], HOU Mei-Ting[b], TAI Bo-Wen[a], AN Yu-Ke[c]

[a] State Key Laboratory of Frozen Soils Engineering, Northwest Institute of Eco-Environment and Resources, Chinese Academy of Science, Lanzhou, 730000, China
[b] China Meteorological Administration Training Centre, Beijing, 100081, China
[c] Gansu Province Transportation Planning, Survey & Design Institute Limited Liability Company, Lanzhou, 730000, China

Received 1 August 2020; revised 4 December 2020; accepted 25 January 2021
Available online 8 February 2021

Abstract

Permafrost in Northeast China is highly sensitive to climate warming. Permafrost degradation significantly affects forest and vegetation ecosystems, as well as the safety of engineering projects and other man-made infrastructures. However, the permafrost change in the region is still unclear. This study uses metrological data from 258 weather stations, alongside reanalysis data, and other environmental data to investigate permafrost degradation and its related environmental impacts in Northeast China from the 1950s to 2010s. Results show that the total permafrost area decreased from 4.8×10^5 to 3.1×10^5 km^2 from the 1950s to the 2010s. The southern limit of permafrost moved 0.1–1.1° northward, and its average elevation rose 160.5 m. During the study period, the degradation of predominantly continuous permafrost, and discontinuous and island permafrost was more pronounced than that of sparsely island permafrost. The south boundary of those three permafrost zones northward by 0–3.4°, 0–5.5° and 0.4–1.1°, the average altitude raised by 339.2 m, 208.3 m, 67.1 m. The permafrost degradation shows the elevation and latitude zonality. Permafrost degradation is mainly caused by the rising of surface temperatures and the impacts of other environmental factors. The snowfall warming the ground of 1.1–10.2 °C in cold seasons and rainfall cooling on surface conditions in warm seasons, those may result in temporal and spatial differences in permafrost degradation. However, there are lack of researches in the impact of environment factors on soil temperatures, moisture and permafrost degradation.

Keywords: Northeast China; Climate warming; Permafrost degradation; Impact of environmental factors

1. Introduction

The permafrost in Northeast China is warmer and thinner than that in high-altitude and high-latitude areas, and is thus highly sensitive to climate warming (Romanovsky et al., 2010; Zhao et al., 2010). Under climate warming, the permafrost in Northeast China thaws easily, increasing the risk of carbon emissions (Yang et al., 2010; Shan et al., 2020), freeze-thaw disasters (Shan et al., 2015; Guo and Wang, 2017), and the safe operation of infrastructures (Tai et al., 2018; Wang et al., 2019). Degradation characteristics of permafrost in Northeast China is similar to that found in southern Russia (He et al., 2009; Chang, 2011; Guo et al., 2018a; Kondratiev, 2016), the permafrost degradation exhibits both latitudinal and altitudinal zonality. The degradation sequence is first on the mountain, then on the valley bottom; first on the sunny slope and then on the shade slope. The impact of environmental effect on permafrost is noticeable (Guo et al., 1981; Zhou et al., 2000; Sun et al., 2007; Jin et al., 2009). Compared with the degradation of high-latitude and high-altitude permafrost, but more significant than the degradation occurring in Western Siberia or the Arctic and Qinghai-Tibet Plateau areas (Jin et al., 2007).

In additional to zonality factors (longitude, latitude and altitude), the distribution and degradation of permafrost in

* Corresponding author.
E-mail address: zhongqionghao@163.com (ZHANG Z.-Q.).
Peer review under responsibility of National Climate Center (China Meteorological Administration).

https://doi.org/10.1016/j.accre.2021.01.006

Northeast China is also closely related with the non-zonality factors (air temperature, snow, precipitation, etc.) (Zhou et al., 2000; He et al., 2009; Chang, 2011; Guo et al., 2018b; Kondratiev, 2016). The southern limit of permafrost was found to be equivalent to the mean annual air temperature (MAAT) of 0 °C and the January temperature of −24 °C for the first time in 1950's (Xin and Ren, 1956). As the MAAT rose from −5 °C to 0 °C, the extent of the permafrost dropped from 80% to 5% (Guo et al., 1981; Akaike,1974). Related results see Reference "Lu et al., 1993". However, results of a more recent equivalent latitude model showed that southern limit of permafrost extended southwards as sparsely island permafrost, with a thickness of less than 1.5 m, when the mean annual surface temperature (MAST) was less than 1.5 °C (Wei et al., 2011).

Changes in the active layer have been found to be dependent upon air temperature conditions in the Northern Da Xing'anling Mountain, and to vary with moisture content, ground surface conditions, and soil type (Wang et al., 1989). Seasonal and annual changes in air temperature alter the thawing and freezing rate and maximum thawing depth of active layer (Wang et al., 1989; Jin et al., 2009). Meanwhile, snow and precipitation directly affect changes in active layer thickness by altering the hydrothermal properties of the active layer (Zhu et al., 2019). The warming effect of snow on the ground surface increases active layer thickness when the snow depth is less than 60 cm (Zhou et al., 1993; Luetschg et al., 2008). Additionally, vegetation can decrease active layer thickness by intercepting snow, reducing solar radiation, and changing the water and heat conditions in the active layer (Chang et al., 2011; Chen et al., 2020). Generally, the active layer thickness under bare ground is considered to be 0.4−0.5 m deeper than under ground with snow and vegetation cover in the Northern Da Xing'anling Mountain (Wang et al., 1989). Furthermore, human activities and urbanization processes alter water and heat exchange conditions, and promote permafrost degradation (Jin et al., 2008; He et al., 2009; Chang et al., 2013; Wang et al., 2019).

Under the influence of climate warming and changing environmental factors, the discussion on the permafrost changes in Northeast China is not comprehensive, especially the spatial−temporal responses of permafrost to climate warming. Local, short-term, or small-scale research in permafrost degradation has proven insufficient in accounting for regional development and broader environmental changes. Research on long-term permafrost change is important to understanding the regional ecological environment, hydrology and carbon cycles, and infrastructure services in Northeast China.

This study employs both long-term temperature change data from the 1950s−2010s extracted from weather stations and reanalysis data to examine permafrost degradation in Northeast China. The response of surface temperature to air temperature and impact of snow cover and precipitation on surface temperature are elaborated. These results can provide important basic data for regional development and engineering design and maintenance in Northeast China under conditions of a warming climate.

2. Data and methods

2.1. Study area

The study area is located in Northeast China (north of 38° N and east of 113°E) (Fig. 1), and is composed of predominantly continuous permafrost, predominantly continuous and island permafrost, sparsely island permafrost, and seasonal frozen soil (Zhou et al., 2000). Within this region, permafrost is mainly distributed in the Da and Xiao Xing'anling Mountains, the northern Songnen Plain, and other regional high mountains located in areas with seasonally frozen soil (e.g., the Changbai Mountains). Compared with high-altitude permafrost and Arctic permafrost, permafrost in Northeast China is thin and warm, and thus particularly sensitive to climate warming.

2.2. Data

2.2.1. Weather station data

Air temperature, precipitation, maximum snow depth, and surface temperature in 1951−2017 were recorded at 258 local weather stations. Ground temperatures above 320 cm in depth were recorded in 1956−2017 at five stations (Jiagedaqi, Hailar, Yichun, Gen'he, Ai'hui; Fig. 1). These data were extracted from a local monthly dataset of ground meteorological elements. Quality control has been performed on the data to ensure integrity, continuity and validity (Xu et al., 2019). The air temperature data is the temperature at a height of 2 m above the ground surface. Before 2005, the surface temperature is the temperature at the surface of the snow cover in winter and at the ground surface in other seasons. After 2005, surface temperature is the temperature at the 0 cm depth (half of the temperature probe was buried in the soil).

From 2003 to 2005, monitoring at meteorological stations data switched from manual to automatic, and the ground temperature observation instruments changed from thermometers to platinum resistance sensors (Xu et al., 2019). These changes resulted in a number of systematic errors. Data is available from 210 sites starting in the 1950s, and 258 sites post-2000. In the permafrost distribution area (north of 45 ^{o}N), over 95% of the available weather data records begin in the 1950s. Therefore, the difference in start time of monitoring does not significantly affect the analysis of permafrost changes.

2.2.2. Reanalyzed data

The current study also makes use of reanalyzed air temperature data from the China meteorological forcing data set (CMFD) (http://data.tpdc.ac.cn/), which was developed by the Data Assimilation and Modeling Center for Tibetan Multi-spheres, Institute of Tibetan Plateau Research, Chinese Academy of Sciences (He et al., 2020). The temporal and spatial resolutions of this dataset were taken every 3 h at increments of 0.1 × 0.1 in longitude and latitude from 1980 to

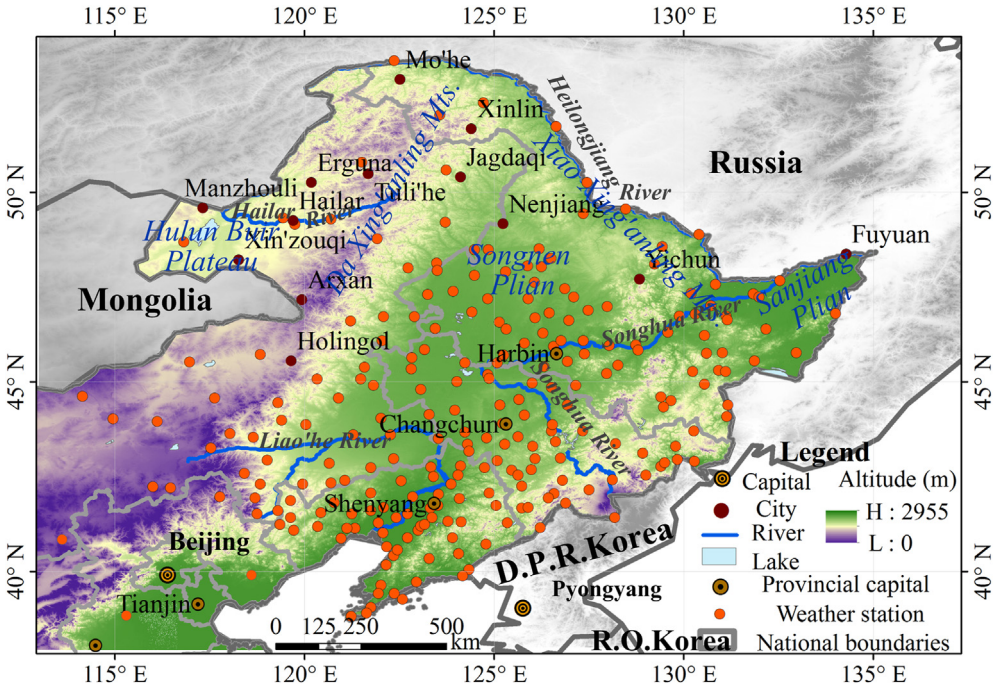

Fig. 1. Distribution of weather stations in Northeast China.

2017. Combined with air temperature data from meteorological stations, CMFD data after 2005 were used to calculate MAST.

2.2.3. DEM data

DEM data was extracted from SRTM1 (http://glovis.usgs.gov/) with 100 m spatial resolution. For outliers, the difference between the center pixel and the mean value of eight adjacent pixels was calculated. When the difference exceeded twice the standard deviation, the data of the center pixel marked outliers. An average value was calculated for an area 100 × 100 pixels around the center pixel. If the difference between the center pixel and the average value of surrounding pixels was less than twice the standard deviation, it was restored to a normal pixel. If it was more than twice the standard deviation, the value was determined to be an outlier. The outliers and no data areas were replaced with GDEM V2, and SRTM3 data. The adjacent pixel interpolation method was used to supplement values where they could not be replaced. Later, stepwise partitioning, projection change, resampling, and 3-dimensional modeling were used to obtain a DEM of 100 m resolution in the study area. The DEM data were then used to analyze topographic conditions and estimate the MAAT and the MAST.

2.3. Methods

2.3.1. Geographically weighted regression (GWR) model

Geographically weighted regression (GWR) is a spatial variable parameter regression model proposed on the basis of local smoothness (Akaike, 1974; Brunsdon et al., 1996). It is an extension of the ordinary linear regression model which embeds the geographic location of the sample data in regression parameters (Ran et al., 2018). The Gauss function, as the core function spatial matrix of the GWR model (Brunsdon et al., 1998), is a continuous monotonic decreasing function representing the weight matrix (W_{ij}) and the bandwidth (d_{ij}) between an estimated point and a measured point.

MAST *in situ* at 258 sites in Northeast China and five independent variables (longitude, latitude, altitude, precipitation, and snow depth) were combined using a GWR model to estimate the MAST with a 100 m resolution in the 1950s–2010s. Longitude, latitude and altitude were used as independent variables. The correlation coefficient between the MAST and the independent variables was 0.93–0.94, and the root mean square error was 0.66–0.75. When independent variables included snow and precipitation, the root mean square error was 0.61–0.86, with the largest margin of error found in the high mountains south of 45°N.

2.3.2. Spatial statistics and clustering

Spatial statistics of classification area and unit and statistical clustering methods were used to analyze changes in altitude, latitude, and temperature in permafrost distribution areas in the 1950s–2010s. The linear regression method was used to analyze the relationship between the MAAT and the ground temperature, and between precipitation/snow cover and ground surface temperature. The study selected a 95% confidence level to assess significance for all statistical analyses.

2.3.3. Classification of thermal state of permafrost

The zoning principle in Zhou et al. (2000) takes into account actual data from frozen ground surveys, weather station data, and topographic characteristics. The first quantitative classification of permafrost in Northeast China was based on

the MAAT and the annual range of air temperature. This classification relies on indicators such as permafrost properties and areal continuity. The continuity of permafrost in Northeast China was found to be less than 90%, with most areas less than 50% (Zhang et al., 2019). The classification presented in Zhou et al. (2000) references the permafrost classification parameters in southern Russia, making it more suitable for local scale analysis than the classification parameters suggested by the International Permafrost Association (Brown et al., 1998).

The southern limit of permafrost is considered to vary within a MAAT range of −1 to 1 °C (Lu et al., 1993), a parameter which reflects the general characteristics of frozen ground in Northeast China. The MAAT was converted into MAST using the linear correlation between MAAT and MAST (Zhang et al., 2019). The zoning principle refers to the results of the empirical model and drilling data (Zhang et al., 2018, 2019), as shown in Table 1.

3. Results

3.1. Temporal and spatial changes of permafrost based on changes in MAST

Fig. 2 shows temporal and spatial changes to the permafrost in Northeast China based on the multi-year average of MAST in the 1950s−2010s. Permafrost is mainly distributed across the Da and Xiao Xing'anling Mountains, Hulun Buir Plateau, and northern Songnen Plain, with sporadic distribution in the Sanjiang Plain, and the high mountainous south of the 45 °N. On the Hulun Buir Plateau, the Songnen Plain, and in the Xiao Xing'anling Mountains, much sparsely island permafrost degraded into seasonally frozen soil, and the southern limit of permafrost moved northward about 0.1°–1.1° from the 1950s−2010s (Fig. 2a−d). In the Da Xing'anling Mountains, and especially the area north of 50°N, the predominantly continuous permafrost had degenerated into discontinuous or sparsely island permafrost, meaning that the distribution range reduced from the 1950s to the 2010s (Fig. 3a). The total area of permafrost changed from 4.8×10^5 km^2 in the 1950s to 3.1×10^5 km^2 in the 2010s, representing a 36.5% reduction in total areal extent of permafrost with a decrease rate of 3.6×10^4 km^2 per decade. The permafrost area reached its minimum in the 2000s, about 2.7×10^5 km^2 (Fig. 2d). The total areas of predominantly continuous permafrost, predominantly continuous and island permafrost, and sparsely island permafrost demonstrated reductions of 90%, 43.4%, 23.8%, respectively, with decrease rates of 0.7×10^4, 1.2×10^4, 0.8×10^4 km^2 per decade (Table 2).

The MAST changed from 3.4 °C in the 1950s to 4.7 °C in the 2010s, increasing by 0.4−1.8 °C in most area. The MAST increased by 1.6−1.8 °C in the northernmost part of study area, 1.4−1.6 °C on the Songnen Plain and the Hulun Buir Plateau, and 1.2−1.4 °C in Da and Xiao Xing'anling Mountain. The MAST change was −0.1–1.2 °C in the mountains above 1000 m (Fig. 2e, f, g, h). Before the 1970s, the MAST increased by 0.4−1.0 °C in permafrost area, 0.7−1.0 °C and 0.5−0.8 °C in the eastern and western areas of the Da Xing'anling Mountains, respectively (Fig. 2f). The MAST increased from 0.8 to 1.1 °C in the area north of 50 °N, and increased from 0.3 to 0.8 °C in the permafrost area south of 50 °N from the 1970s−1990s (Fig. 2g). The MAST decreased in the area north of 45 °N after the 1990s. Permafrost degradation mainly occurred before 1990s as the MAST increased (Fig. 2). Decrease of permafrost area and northward shift of the southern boundary was almost consistent with the area of increasing MAST (Fig. 3). As such, it can be concluded that the spatio-temporal increase in MAST is one of the main reasons for the differential degradation of permafrost.

3.2. Elevational and latitudinal zonality of permafrost degradation

As the same as elevational and latitudinal zonality of permafrost distribution (Zhou et al., 2000), permafrost degradation represents altitudinal and latitudinal zonality. In the 1950s, predominantly continuous permafrost was mainly distributed from 53.4°–47.7°N within the range of 5.7°, but had compressed to 52.7°–51.3°N (range of 1.4°) by the 2000s. The predominantly continuous and island permafrost mainly distributed from 53.5°–42°N in 1950s, the southern boundary was close to 47.7 °N in 2000s. In contrast, the latitudinal range of the sparsely island permafrost extended 0.7° northward in the 1950s−2010s, distributed from 53.5°–41.7°N in 2010s (Fig. 4b). In 1950s−2010s, the south boundary of those three permafrost zones northward by 0−3.4°, 0–5.5° and 0.4−1.1°.

For the region of 53.5°−39.0°N, the average altitude of permafrost distribution varied from 702.2 m in the 1950s to 862.7 m in the 2000s (Rose by 160.5 m), indicating that permafrost degraded significantly towards higher altitudes. However, there were noticeable differences in the extent of degradation between permafrost zones. From the 1950s−2010s, the average altitude varied from 851.7 m to

Table 1
Classification system used to assess the degradation of permafrost (modified according to Zhou et al. (2000)).

Permafrost zone	MAAT (°C)	MAST (°C)	Mean annual ground temperature (°C)	Area extent of permafrost (%)	Estimated permafrost thickness (m)
Predominantly continuous permafrost	< −5	< −3.7	−4–0	70−80	50−100
Predominantly continuous and island permafrost	−5 to −3	−3.7 to −1.6	−1.5–2	30−70	20−50
Sparsely island permafrost	−3 to −1	−1.6−0.4	−1–3	5−30	5−20
Isolated patches permafrost	−1–1	0.4−1.5	0−4	<5	−

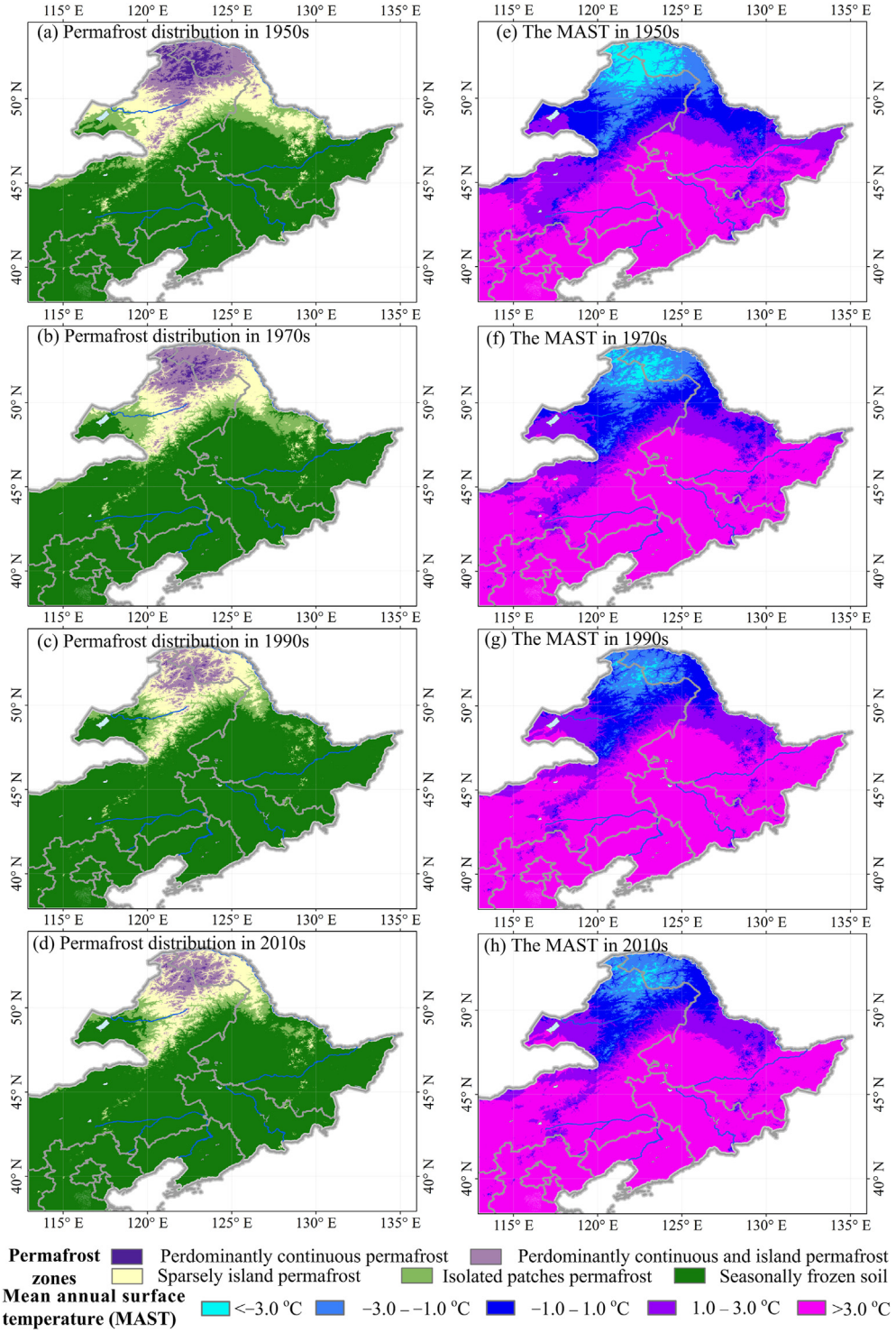

Fig. 2. Spatial distribution of different permafrost zones (a–d) and mean annual surface temperature (MAST) (e–h) in Northeast China during the 1950s–2010s.

1191.9 m, rose by 339.2 m in the predominantly continuous permafrost area. On the other hand, the average altitude varied from 677.9 m to 886.2 m, rose by 203.8 m in predominantly continuous and island permafrost area (Fig. 4a). The average altitude of the sparsely island and isolated patches permafrost rose by 67.1 m and 43.6 m in the 1950s–2010s.

It is worth noting that permafrost degradation in high mountain areas (altitude above 1000 m) has been slower than that in plains due to differential rise rates for both MAAT and MAST. From the 1950s–2010s, the rise rate of MAAT was about 0.2 °C per decade in altitude ranges of 100–1000 m and 0.1–0.2 °C per decade above 1000 m (Fig. 5b). However, the

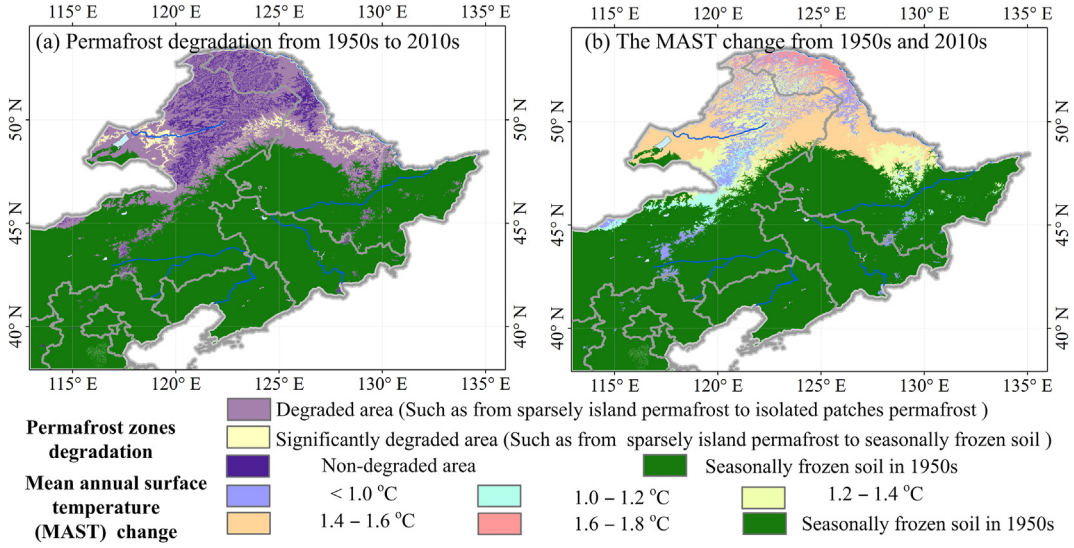

Fig. 3. Permafrost degradation (a) and MAST rise (b) in Northeast China during the 1950s–2010s.

rise rate of the MAST decreases with an increase in altitude (Fig. 5a). Differences in the MAST and MAAT rise with altitude range result in spatial–temporal differences in permafrost degradation. The altitudes in the southern part of Da Xing'anling Mountains and the high mountains south of 45° N are greater than 1000 m. Therefore, the northward shift of the southern boundary of the predominantly continuous permafrost, and predominantly continuous and island permafrost was greater than that of sparsely island permafrost.

4. Discussion

4.1. The response of ground temperature to MAAT changes

Permafrost degradation is mainly caused by climate warming. Rising air temperatures result in rising permafrost temperatures, particularly in soil temperatures within the active layer (Jin et al., 2007). Fig. 6 shows that the change trends of ground temperatures at different depths were consistent with changes in MAAT from 1956 to 2017. Ground temperature at the different depths can be seen to be linearly related to MAAT with a correlation coefficient of 0.59–0.63, which is less than that suggested for the period from 1951 to 1980 (R^2 = 0.93) (Zhou et al., 1996). This finding indicates that changes in ground temperature were mainly driven by change in air temperature before 1980, and may have be influenced primarily by the air temperature and other environmental factors (such as snow, precipitation, forest fires, human activities) after 1980 (Jin et al., 2007). From the 1950s to the 2010s, the rise of MAAT was more than 1.5 °C in the Da Xing'anling Mountains (below 1000 m), the Hulun Buir Plateau, the Songnen Plain, and the northern part of the Xiao Xing'anling Mountains. In the southern area of the 45° N, the increase in the MAAT was less than 1.1 °C. The regions which demonstrated rises in MAAT are consistent with regions demonstrating rising ground temperatures and permafrost degradation (Fig. 3).

4.2. Impact of snow cover on mean annual ground surface temperature(MAGST)

Because of its high reflectivity, high emissivity, and low thermal conductivity, snow cover can manifest insulation and warming effects (Zhang, 2005). The MAGST is thus closely related with the time of first snow day and melt day, the snow cover period, snow thickness, and the density and composition of snow cover (Ling and Zhang, 2003; Luetschg et al., 2008; Zhong et al., 2018). Fig. 7 shows that the temperature difference between the top and the bottom of the snow cover increases with maximum snow depth by month (Fig. 7a) and during the snow season (all months with snow, Fig. 7b).

Table 2
Area and change rate statistics for the permafrost in Northeast China since the 1950s.

Permafrost zone	Area (10^4 km^2)							Chang rate (10^4 km^2 per decade)
	1950s	1960s	1970s	1980s	1990s	2000s	2010s	
Predominantly continuous permafrost	3.9	4.1	1.4	1.3	0.3	0.2	0.4	−0.7
Predominantly continuous and island permafrost	12.3	12.1	10.2	9.9	6.3	5.2	6.9	−1.2
Sparsely island permafrost	17.6	17.1	14	14.6	13.4	12.9	13.4	−0.8
Isolated patches permafrost	14.2	14.2	12.6	13.1	9.6	9.1	9.7	−1.0
Total	48.1	47.6	38.1	38.8	29.6	27.4	30.5	−3.6

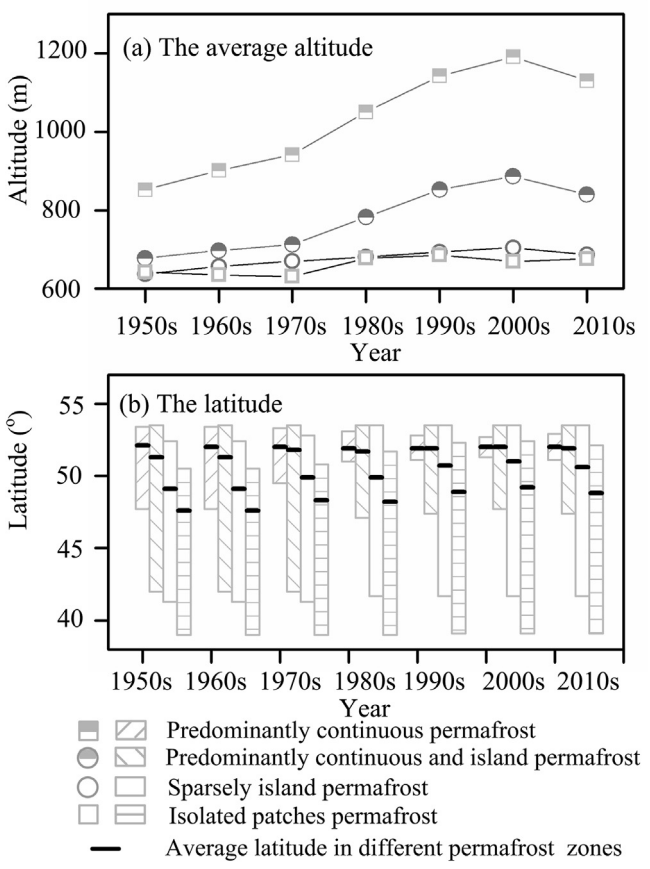

Fig. 4. Changes in the (a) altitudinal and (b) latitudinal ranges of different permafrost zones in Northeast China during the 1950s–2010s.

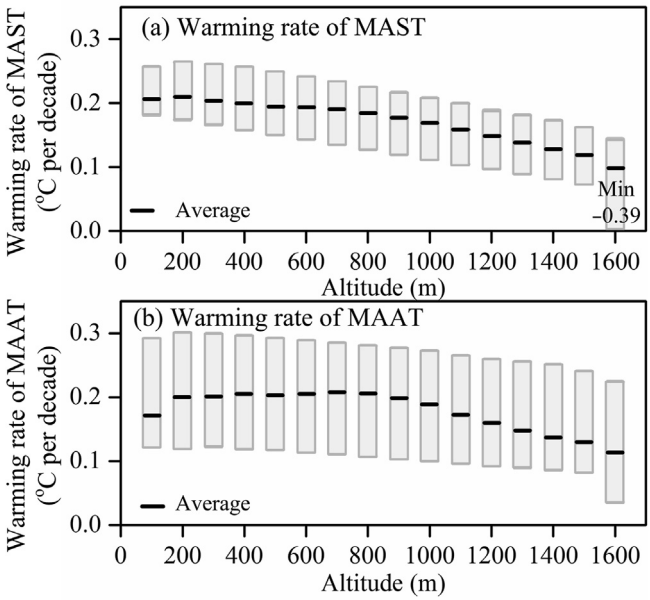

Fig. 5. Warming rates of the (a) MAST and (b) MAAT at different elevation intervals during the 1950s–2010s.

Meanwhile, the mean monthly surface temperature beneath the snow cover and the ground temperature within active layer increase with maximum snow depth (Fig. 7c and d). Snow cover caused increases in ground surface temperature ranging from 1.1 to 10.2 °C during cold seasons. These results indicate that the warming effect of snow cover on surface temperature could cause ground temperature increase, leading to the thinning of the active layer, and the degradation of permafrost (Zhang, 2005; Jin et al., 2007).

In our study areas, the snow depth was mostly 15–40 cm (Fig. 7). The snow cover is thicker in the northeastern area than in the southwestern area, and thicker in the mountains and tableland to the north of 50°N than on the plains (Zhong et al., 2018; Bo, 2019). Therefore, the warming effect of snow on MAGST is closely linked to the significant permafrost degradation observed in the Xiao Xing'anling Mountains and the area with thick snow cover north of 50°N.

4.3. Impact of precipitation on MAGST

The degradation of permafrost has been found to be closely related to wet/dry conditions in the soil layer (Boike et al., 2016). This is because precipitation infiltration increases the soil water content, resulting in an increase to the thermal conductivity of the soil layer. If surface water dissipates heat primarily through evapotranspiration, precipitation will promote the thinning of the active layer and increase the ground temperature of permafrost. However, if most of the precipitation becomes surface runoff, the impact of precipitation is conducive to the development of permafrost (Subin et al., 2013; Hotaek et al., 2015; Zhang et al., 2017). Fig. 8 shows that ground surface temperature is more noticeably affected by precipitation in the wet season than annual precipitation. With rainfall increase, mean ground surface temperature will decrease between 1.0 and 3.5 °C in the wet season (all months with rainfall greater than 0.1 mm). In terms of the relationship between climate warming and precipitation, it can be seen that while snowfall may increase ground surface temperatures in the cold season (Huang et al., 2012), rainfall can decrease ground surface temperatures in the warm season. Therefore, regional, seasonal differences in precipitation may result in the spatial differences in permafrost degradation. In addition, rainfall infiltration can affect soil moisture in the active layer or in the supra-permafrost subaerial talik (Zhang et al., 2017). However, studies on soil moisture in Northeast China are lacking. In central Siberia, precipitation increases the soil moisture and temperature in the active layer, induces the degradation of permafrost, and possibly lead to the fall or mortality (Iijima et al., 2010, 2014).

4.4. The impact of other environmental factors on permafrost degradation

At a local scale, change of environmental factors, for example, vegetation, forest fires, and urbanization, would impact permafrost degradation (Cheng, 2003). In Northeast China, vegetation can decrease the average ground surface temperature by 0.6–4.9 °C in summer, and reduce ground temperature by at least 1.6 °C in winter (Jin et al., 2008; Chang, 2011). Meanwhile, forest fires drastically increase

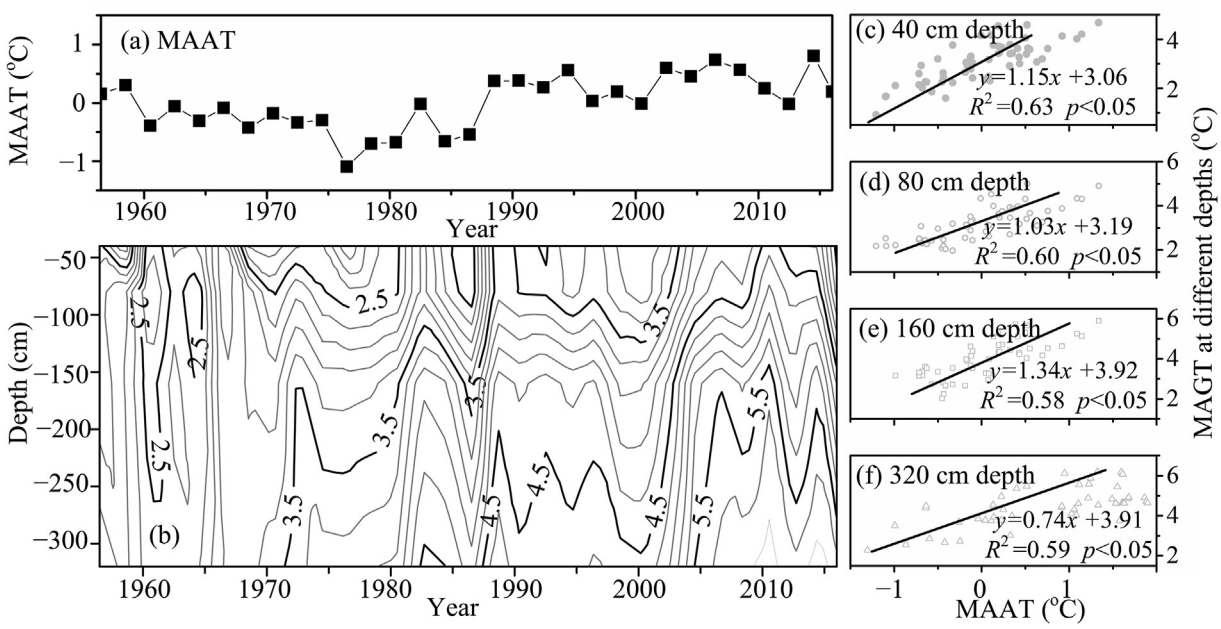

Fig. 6. Changes in (a) MAAT and (b) ground temperatures (°C) at different depths and their correlation (c−f) in Northeast China during the 1950s−2010s.

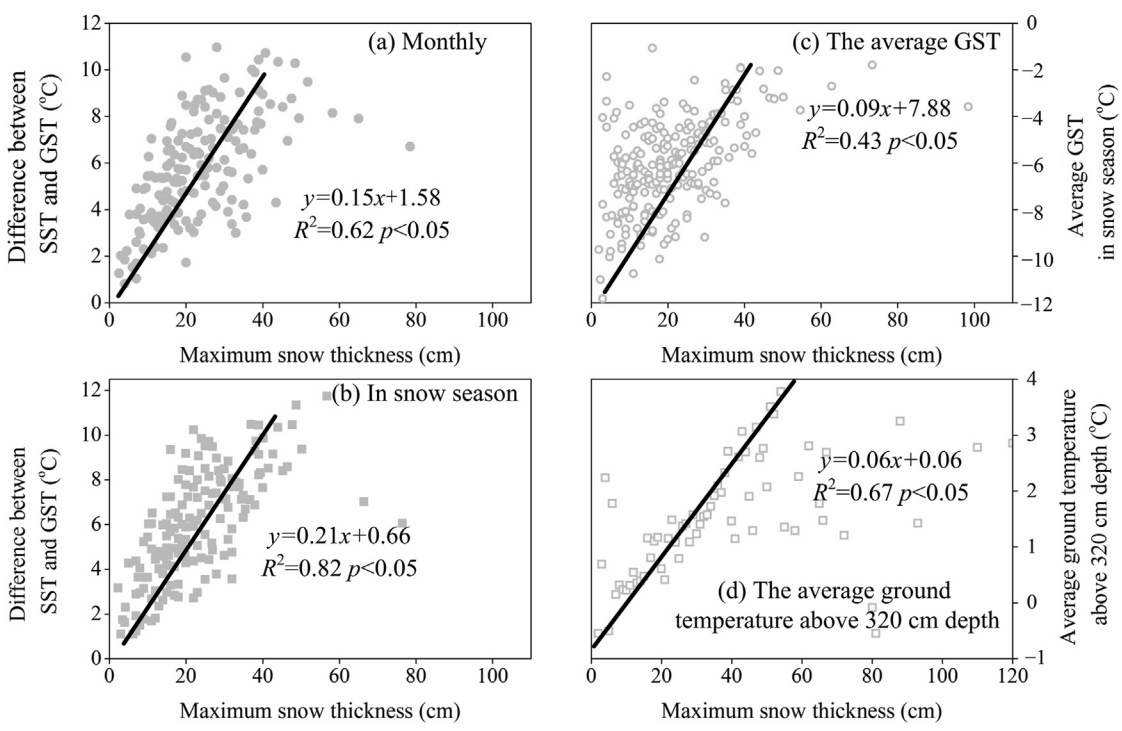

Fig. 7. Insulation (a, b) and warming effect (c, d) of snow cover in 2005−2017 in Northeast China (GST: ground surface temperature; SST: snow surface temperature).

ground surface temperatures, resulting in increases in active layer thickness (Li et al., 2019). The ground surface temperature in a given burn area in July has been found to be about 14 °C greater than in unburned areas. Eight years after a forest fire, the mean annual ground temperature had increased by 2.1 °C in the A'long area of the Da Xing'anling Mountains (Li et al., 2019). Moreover, urbanization and construction have also changed the nature of the ground surface, increasing the mean average ground temperature and deepening the permafrost table (Wang et al., 2016). Since the 1970s, the permafrost table has dropped about 124−388 cm in the urban area of Mo'he, compared to only 17−55 cm in the suburbs (Lu, 2018). In addition, the development of peat bogs has been conducive to the survival of permafrost (Anisimov and Beloloutskaia,

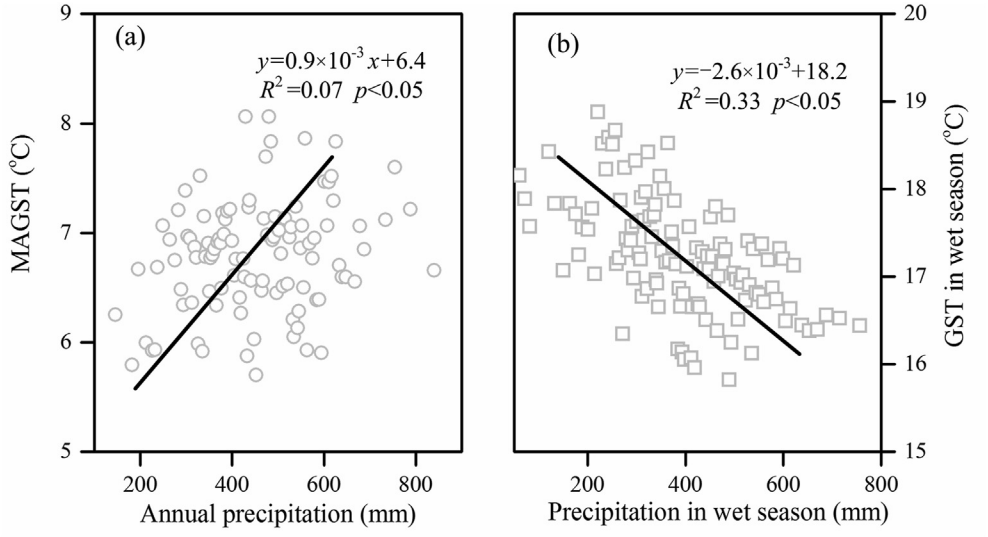

Fig. 8. The annual (a) and seasonal (b) warming and the cooling effects of precipitation on ground surface temperature (GST) in 2005−2017 in Northeast China.

2003; Jin et al., 2008). Geological conditions, quaternary situation, and water content in shallow soils are further factors affecting permafrost degradation in Northeast China (Wang et al., 1989; Jin et al., 2007; Boike et al., 2016). However, there is little relevant research at present. More targeted studies are required to fully assess the impact of a range of environmental factor on permafrost degradation.

5. Conclusions

Under the influence of climate warming and changing environmental factors, the permafrost in Northeast China has been degrading in the 1950s−2010s. This study analyzed the permafrost area reduction and its zonality of permafrost degradation, discussed the effect of environmental factors, such as MAAT, snow and precipitation.

(1) The total permafrost area decreased from 4.8 × 10^5 km^2 in the 1950s to 3.1 × 10^5 km^2 in the 2010s, at a rate of 3.6 × 10^4 km^2 per decade. The plains area, the northernmost part of the study area, the Hulun Buir Plateau, and the northern part of the Xiao Xing'aning Mountains are home to the most significant areas of permafrost degradation.

(2) The permafrost degradation shows the elevational and latitudinal zonality. The southern limit of permafrost moved 0.1°–1.1° northward in the 1950s−2010s, and its average altitude rose by 160.5 m. The boundaries of predominantly continuous permafrost, predominantly continuous and island permafrost, and sparsely island permafrost moved 0–3.4°, 0–5.5° and 0.4−1.1° northward, respectively. It is worth noting that predominantly continuous permafrost moved 0.5° southward in the northern part of Da Xing'anling Mountains. Average altitudes for these three permafrost zones rose by 339.2 m, 208.3 m, and 67.1 m, respectively.

(3) MAST in Northeast China demonstrates a prominent, yet spatially diverse rising trend. The MAST changed from 3.4 °C in the 1950s to 4.7 °C in 2010s. The area of permafrost degradation considered in the study was almost consistent with the area of MAST increase. Snow cover caused increases in surface temperature about 1.1−10.2 °C during cold seasons, but precipitation caused decreases ranging from 1.0 to 3.5 °C during warm seasons. The impact of snow cover on surface temperature in cold seasons and of precipitation in warm seasons may cause spatiotemporal differences in permafrost degradation.

Declaration of competing interest

The authors declare no conflict of interests.

Acknowledgments

We would like to express our sincerest gratitude to the anonymous four unidentified reviewers for providing us with constructive and insightful comments and suggestions. The study was financially supported by the National Natural Science Foundation of China (41771074, 41690144), foundation for excellent youth scholars of Northwest Institute of Eco-Environment and Resources, Chinese Academy of Sciences (FEYS2019002).

References

Akaike, H., 1974. A new look at the statistical model identification. IEEE Transactions on. Automatic Control 19 (6), 716–723.

Anisimov, O., Beloloutskaia, M., 2003. Feedbacks in climate-permafrost-vegetation system: Predictive Modeling Approach. American Geophysical Union, Fall Meeting, San Francisco.

Bo, A., 2019. Snow depth in Northeast China from 1980 to 2012 effect on soil moisture. Harbin Normal University (Chinese).

Boike, J., Grau, T., Heim, B., et al., 2016. Satellite-derived changes in the permafrost landscape of central Yakutia, 2000−2011: wetting, drying, and fires. Global Planet. Change 139, 116−127. https://doi.org/10.1016/j.gloplacha.2016.01.001.

Brown, J., Ferrians, O.J., Heginbottom, J.A., et al., 1998. Circum-arctic map of permafrost and ground ice conditions (revised 2001). National Snow and Ice Data Center. Digital media, Boulder.

Brunsdon, C., Fotheringham, A.S., Charlton, M.E., 1996. Geographically weighted regression: a method for exploring spatial nonstationarity. Geogr. Anal. 28 (4), 281−298. https://doi.org/10.1111/j.1538-4632.1996.tb00936.x.

Brunsdon, C., Fotheringham, S., Charlton, M., 1998. Geographically weighted regression. J. Roy. Stat. Soc. D 47, 431−443.

Chang, X.L., 2011. Thermal effect of vegetation and snow cover on the underlying permafrost and soil in the active layer in the northern Da Xing'anling Mountains, Northeastern China. Cold and Arid Regions Environmental and Engineering Research Institute, CAS (Chinese).

Chang, X.L., Jin, H.J., Yu, S.P., et al., 2011. Influence of vegetation on frozen ground temperatures the forested area in the Da Xing'anling Mountains, Northeastern China. Acta Ecol. Sin. 31 (18), 5138−5147 (Chinese).

Chang, X.L., Jin, H.J., He, R.X., et al., 2013. Review of permafrost monitoring in the northern Da Hinggan mountains, Northeast China. J. Glaciol. Geocryol. 35 (1), 93−100 (Chinese).

Chen, S.S., Zang, S.Y., Sun, L.L., 2020. Characteristics of permafrost degradation in Northeast China and its ecological effects: a review. Sci. Cold Arid Reg. 12 (1), 1−11. https://doi.org/10.3724/SP.J.1226.2020.00001.

Cheng, G.D., 2003. Influences of local factors on permafrost occurrence and their implications for Qinghai-Xizang Railway design. Sci. China E D 33 (6), 602−607. https://doi.org/10.1007/BF02893300.

Guo, D.L., Wang, H.J., 2017. Permafrost degradation and associated ground settlement estimation under 2 °C global warming. Clim. Dynam. 49, 2569−2583. https://doi.org/10.1007/s00382-016-3469-9.

Guo, D.L., Li, D., Hua, W., 2018a. Quantifying air temperature evolution in the permafrost region from 1901 to 2014. Int. J. Climatol. 38, 66−76. https://doi.org/10.1002/joc.5161.

Guo, D.X., Wang, S.L., Lu, G.W., et al., 1981. Division of permafrost regions in da Xiao hinggan ling Northeast China. J. Glaciol. Geocryol. 3 (3), 1−9 (Chinese).

Guo, W.C., Liu, H.Y., Anenkhonov, O.A., et al., 2018b. Vegetation can strongly regulate permafrost degradation at its southern edge through changing surface freeze-thaw processes. Agric. For. Meteorol. 252, 10−17. https://doi.org/10.1016/j.agrformet.2018. 01.010.

He, J., Yang, K., Tang, W., et al., 2020. The first high-resolution meteorological forcing dataset for land process studies over China. Sci. Data 7, 25. https://doi.org/10.1038/s41597-020-0369-y.

He, R.X., Jin, H.J., Chang, X.L., et al., 2009. Degradation of permafrost in the northern part of northeastern China: present state and causal analysis. J. Glaciol. Geocryol. 31, 829−834 (Chinese).

Hotaek, P., Youngwook, K., John, S.K., 2015. Widespread permafrost vulnerability and soil active layer increases over the high northern latitudes inferred from satellite remote sensing and process model assessments. Remote Sens. Environ. 12 (4), 349−358. https://doi:10.1016/j.rse.2015.12.046.

Huang, J., Guan, X., Ji, F., 2012. Enhanced cold-season warming in semi-arid regions. Atmos. Chem. Phys. 12 (12), 5391−5398. http://doi:10.5194/acp-12-5391-2012.

Iijima, Y., Fedorov, A.N., Park, H., et al., 2010. Abrupt increases in soil temperatures following increased precipitation in a permafrost region, central Lena River basin, Russia. Permafr. Periglac. Process. 21 (1), 30−41. https://doi.org/10.1002/ppp.662.

Iijima, Y., Ohta, T., Kotani, A., et al., 2014. Sap flow changes in relation to permafrost degradation under increasing precipitation in an eastern Siberian larch forest. Ecohydrology 7 (2), 177−187. https://doi.org/10.1002/eco.1366.

Jin, H.J., Yu, Q.H., Lv, L.Z., et al., 2007. Degradation of permafrost in the Xing'anling Mountains, northeastern China. Permafr. Periglac. Process. 18, 245−258. https://doi.org/10.1002/ppp.589.

Jin, H.J., Zhang, J.M., Yu, Q.H., et al., 2008. Identification and Mitigation of Frost Hazards along the China-Russia Oil Pipeline. The Proc., 9th Int. Conf. On Permafrost, Alaska. University of Alaska Fairbanks, pp. 845−850.

Jin, H.J., Wang, S.L., Lv, L.Z., et al., 2009. Features of permafrost degradation in hinggan mountains northeastern China. Sci. Geogr. Sin. 29 (2), 68−74 (Chinese).

Kondratiev, S.V., 2016. Deformations of the transbaikal part of the federal highway amur on Chita-Khabarovsk sections of icy permafrost soils: causes and solutions. Transbaikal State University, Russia.

Li, X.Y., Jin, H.J., He, R.X., et al., 2019. Effects of forest fires on the permafrost environment in the northern Da Xing'anling Mountain NE, China. Permafr. Periglac. Process. 30, 163−177. https://doi.org/10.1002/ppp.2001.

Ling, F., Zhang, T.J., 2003. Impact of the timing and duration of seasonal snow cover on the active layer and permafrost in the Alaskan Arctic. Permafr. Periglac. Process. 14, 141−150. https://doi.org/10.1002/ppp.445.

Lu, G.W., Weng, B.L., Guo, D.X., 1993. The geographic boundary of permafrost in the Northeast of China. J. Glaciol. Geocryol. 15, 214−218 (Chinese).

Lu, Y., 2018. Study on the Change of Permafrost in Urban Environment: a Case Study of Mo'he County. Northwest Institute of Eco-Environmental and Resources Chinese Academy of Sciences, Lanzhou.

Luetschg, M., Lehning, M., Haeberli, W.A., 2008. Sensitivity study of factors influencing warm/thin permafrost in the Swiss Alps. J. Glaciol. 54 (187), 696−704. https://doi.org/10.3189/002214308786570881.

Ran, Y.H., Li, X., Cheng, G.D., 2018. Climate warming over the past half century has led to thermal degradation of permafrost on the Qinghai−Tibet Plateau. Cryosphere 12, 595−608. https://doi.org/10.5194/tc-12-595-2018.

Romanovsky, V.E., Smith, S.L., Christiansen, H.H., 2010. Permafrost thermal state in the polar Northern Hemisphere during the international polar year 2007−2009: a synthesis. Permafr. Periglac. Process. 21, 106−116. https://doi.org/10.1002/ppp.689.

Shan, W., Zhao, G.H., Guo, Y., et al., 2015. The impact of climate change on the landslides in the southeastern of high-latitude permafrost regions of China. Front. Earth Sci. 3 (7), 1−11. https://doi.org/10.3389/feart.2015.00007.

Shan, W., Xu, Z.C., Guo, Y., et al., 2020. Geological methane emissions and wildfire risk in the degraded permafrost area of the Xiao Xing'an Mountains, China. Sci. Rep. 10, 21297. https://doi.org/10.1038/s41598-020-78170-z.

Subin, Z.M., Koven, C.D., Riley, W.J., et al., 2013. Effects of soil moisture on the responses of soil temperatures to climate change in cold regions. J. Clim. 10, 3139−3158. https://doi.org/10.1175/JCLI-D-12-00305.1.

Sun, G.Y., Yu, S.P., Wang, H.X., 2007. Causes south borderline and subareas of permafrost in Da and Xiao Hinggan mountains. Sci. Geogr. Sin. 27 (1), 68−74 (Chinese).

Tai, B.W., Liu, J.K., Yue, Z.R., et al., 2018. Effect of sunny shady slopes and strike on thermal regime of subgrade along a high-speed railway in cold regions. China. Eng. Geol. 232, 182−191. https://doi.org/10.1016/j.enggeo.2017.09.002.

Wang, F., Li, G.Y., Ma, W., et al., 2019. Pipeline−permafrost interaction monitoring system along the China−Russia crude oil pipeline. Eng. Geol. 254, 113−125. https://doi.org/10.1016/j.enggeo.2019.03.013.

Wang, J.C., Guo, D.X., Huang, Y.Z., et al., 1989. A study on seasonally thawed layer in the basin of Huola River in northern Da Hinggan Ling. J. Glaciol. Geocryol. 11 (3), 203−214 (Chinese).

Wang, Y.P., Jin, H.J., Li, G.Y., 2016. Investigation of the freeze-thaw states of foundation soils in permafrost areas along the China-Russia Crude Oil Pipeline (CRCOP) route using ground-penetrating radar (GPR). Cold Reg. Sci. Technol. 126, 10−21. https://doi.org/10.1016/j.coldregions.2016.02.013.

Wei, Z., Jin, H.J., Zhang, J.M., et al., 2011. Prediction of permafrost changes in Northeastern China under a changing climate. Sci. China Earth Sci. 54 (6), 924−935. https://doi: 10.1007/s11430-010-4109-6.

Xin, K.D., Ren, Q.J., 1956. Permafrost distribution in northeastern China. Geol Knowledge (10), 15−18.

Xu, W.H., Sun, C., Zuo, J.Q., et al., 2019. Homogenization of monthly ground surface temperature in China during 1961−2016 and performances of GLDAS reanalysis products. J. Clim. 32, 1121−1135. https://doi.org/10.1175/JCLI-D-18-0275.1.

Yang, Z.P., Ou, Y.H., Xu, X.L., et al., 2010. Effects of permafrost degradation on ecosystems. Acta Ecol. Sin. 30, 33−39. https://doi.org/10.1016/j.chnaes.2009.12.006.

Zhang, T., 2005. Influence of the seasonal snow cover on the ground thermal regime: an overview. Rev. Geophys. 43 (4), RG4002. https://doi.org/10.1029/2004RG000157.

Zhang, Z.Q., Wu, Q.B., Gao, S.R., et al., 2017. Response of the soil hydrothermal process to difference underlying conditions in the Beiluhe permafrost region. Environ. Earth Sci. 76, 194. https://doi.org/10.1007/s12665-017-6518-8.

Zhang, Z.Q., Wu, Q.B., Xun, X.Y., et al., 2018. Climate change and the distribution of frozen soil in 1980−2010 in northern Northeast China. Quat. Int. 467, 230−241. https://doi.org/10.1016/j.quaint.2018.01.015.

Zhang, Z.Q., Wu, Q.B., Xun, X.Y., et al., 2019. Spatial distribution and changes of Xing'an permafrost in China over the past three decades. Quat. Int. 523, 16−24. https://doi.org/10.1016/j.quaint.2019.06.007.

Zhao, L., Wu, Q.B., Marchenko, S.S., et al., 2010. Thermal state of permafrost and active layer in central asia during the international polar year. Permafr. Periglac. Process. 21 (2), 198−207. https://doi.org/10.1002/ppp.688.

Zhong, X.Y., Zhang, T.J., Kang, S.C., et al., 2018. Spatiotemporal variability of snow depth across the Eurasian continent from 1966 to 2012. Cryosphere 12, 227−245. https://doi.org/10.5194/tc-12-227-2018.

Zhou, Y.W., Guo, D.X., Qiu, G.Q., 2000. Geocryology in China. Science Press, Beijing (Chinese).

Zhou, Y.W., Liang, L.H., Guo, Z.W., et al., 1993. Effect of forest fire on hydrothermal regime of frozen ground, the Northern part of Da Hinggan Ling. J. Glaciol. Geocryol. 15 (1), 17−26 (Chinese).

Zhou, Y.W., Wang, Y.X., Gao, X.W., et al., 1996. Ground temperature, permafrost distribution and climate warming in Northeastern China. J. Glaciol. Geocryol. 18, 139−147 (Chinese).

Zhu, X.F., Wu, T.H., Zhao, L., et al., 2019. Exploring the contribution of precipitation to water within the active layer during the thawing period in the permafrost regions of central Qinghai-Tibet Plateau by stable isotopic tracing. Sci. Total Environ. 661, 630−644. https://doi.org/10.1016/j.scitotenv.2019.01.064.